Article

Investigation of Site-Specific Wind Field Parameters and Their Effect on Loads of Offshore Wind Turbines

Benedikt Ernst * and Jörg R. Seume

ForWind-Center for Wind Energy Research, Institute of Turbomachinery and Fluid Dynamics, Leibniz Universität Hannover, Appelstrasse 9, Hannover 30167, Germany;
E-Mail: seume@tfd.uni-hannover.de

* Author to whom correspondence should be addressed; E-Mail: ernst@tfd.uni-hannover.de;
Tel.: +49-511-762-2734; Fax: +49-511-762-3997.

Abstract: The main contributing factors to unsteady loading of Offshore Wind Turbines (OWT) are wind shear, turbulence, and waves. In the present paper, the turbulence intensity and the wind shear exponent are investigated. Using data from the FINO 1 research platform, these parameters are analyzed and compared with the proposed wind field parameters in the IEC standard 61400-3. Based on this analysis, aeroelastic simulations are performed to determine the effect of wind field parameters on the fatigue and the extreme loads on the rotor blades. For the investigations, the aeroelastic model of a 5 MW OWT is used with a focus on design load cases in an operating state (power production). The fatigue loads are examined by means of the damage-equivalent load-range approach. In order to determine the extreme loads with a recurrence period of 50 years, a peak over threshold extrapolation method and a novel method based on average conditional exceedance rates are used. The results show that the requirements of the IEC standard are very conservative for the design of the rotor blades. Therefore, there could be a large optimization potential for the reduction of weight and cost of the rotor blades.

Keywords: turbulence intensity; wind shear exponent; fatigue loads; extreme loads

1. Introduction

Aeroelastic simulations are performed to design Offshore Wind Turbines (OWT). The turbulence intensity and the wind shear exponent are essential input parameters of the wind field for these simulations. In order to consider these and to reach acceptable reliability and safety levels, there are standards and guidelines for the design of OWTs, e.g., IEC standard 61400-3 "Design Requirements of Offshore Wind Turbines" [1]. There are some more standards and guidelines that tend to give general procedures for safe design, but none of them are very specific [2]. Therefore, probabilistic methods are required for developing a cost optimized OWT with high reliability and low probabilities of failure. With these methods, it is also possible to adjust the safety requirements of the design to specific sites and to calculate individual failure probabilities for OWTs [3].

The IEC standards 61400-1 and 61400-3 [1,4] require to determine the extreme loads in an operating state with a recurrence period of 50 years by statistical extrapolation. In addition to the standards, there are several publications dealing with statistical extrapolation methods. The methods identified by [5] can generally be divided into four groups: peak extrapolation methods, process methods, Inverse First-Order Reliability Methods (IFORM), and methods based on Average Conditional Exceedance Rates (ACER). Peak extrapolation methods use extracted peaks from simulated time series. Local or short-term distributions are fitted to these extracted peaks for a given environmental state. In order to yield a long-term distribution, the short-term distributions are integrated over all environmental states. By means of extrapolating the long-term distribution, the characteristic extreme load with a desired recurrence period is obtained. The way how these peaks are extracted and the selection of the fitting distribution function for the extracted peaks are very important. In the literature, several approaches are investigated [6–12]. Process methods describe the time series as a random process. For this, the first four statistical moments—mean value, standard deviation, skewness and kurtosis—as well as a mean crossing rate of the observed time series are used [11,13]. Another type of extrapolation methods uses an inverse reliability approach. These methods transform the physical environmental variables (e.g., wind speed, turbulence intensity, wave hight) into random variables in the standard normal space. The inverse first-order reliability method, which is based on the Environmental Contours (EC) method, is presented in [6,14]. For example, the EC method has been used by [15,16]. A relatively new extrapolation method, which is based on the mean level upcrossing rate function, was proposed by Naess and Gaidai [17]. In order to account for dependence effects in the data time series, the method was improved by introducing the concept of average conditional exceedance rates [18]. This was then used by Toft *et al.* [5] to examine extreme loads for wind turbines.

The objective of the present paper is to show the effect on the fatigue and extreme loads of an OWT for site-specific wind field parameters compared with the requirements defined in the IEC standard 61400-3 [1]. For this purpose, the turbulence intensity and the wind shear exponent are analyzed at the FINO 1 research platform, which are based on 10 min mean wind data. The fatigue loads are determined by means of the damage-equivalent load-range approach. In order to examine the extreme loads of the OWT, which may occur under different wind conditions, statistical extrapolation methods are used. The IEC standards [1,4] suggest the peak extrapolation method or the IFORM. Typically, only a limited number of simulation time series are available. This implies a significant uncertainty on the extrapolated

loads. Methods based on exceedance rates have a lower uncertainty compared with commonly used peak extrapolation methods [5]. In addition to a peak over threshold method, the method based on average conditional exceedance rates is used to determine the extreme loads. Although the IFORM is an efficient and accurate method [6], it requires specially created input configurations, e.g., of wind speed, turbulence intensity, and wave heights. Because of these requirements, IFORM is not used in the present project.

In the first part of this paper, the required wind field parameters in the IEC standard 61400-3 [1] are reviewed and the corresponding results of the analyzed FINO 1 measurements are presented. In the second part, their effects on the fatigue and extreme loads of a 5 MW OWT model are shown.

2. Wind Field Parameters

2.1. Wind Field Parameters in the IEC Standard 61400

In the IEC standard 61400-1 [4], wind turbine sites are categorized in different classes, according to typical mean wind speeds and turbulence intensities. Besides the annual mean wind speeds $\bar{v}$, Table 1 shows the expected turbulence intensity I_{15} at $15\,\mathrm{m/s}$ wind speed. These parameters do not represent specific sites but they can be generally used during the design process of wind turbines.

Table 1. Wind turbine classes according to IEC 61400-1 [4].

WT class		I	II	III
$\bar{v}$ [m/s]		10	8.5	7.5
A	I_{15} [-]		0.16	
B	I_{15} [-]		0.14	
C	I_{15} [-]		0.12	

The turbulence intensity I is defined as the standard deviation σ_v of the horizontal wind speed related to the mean wind speed v:

$$I = \frac{\sigma_v}{v} \tag{1}$$

In the IEC standards 61400-1 and -3 [1,4], several Design Load Cases (DLC) are defined for Offshore Wind Turbines (OWT). In the present study, the focus is on the turbine response in an operating state and especially DLC 1.1 and DLC 1.2 are examined. Both are defined for normal operation conditions between the cut-in and cut-out wind speed ($v_{in} \leq v \leq v_{out}$) and are used to analyze extreme loads (DLC 1.1) and fatigue loads (DLC 1.2). In the simulations of both DLC the Normal Turbulence Model (NTM) has to be used, which describes the standard deviation depending on the wind speed at hub height v_{hub} and the reference turbulence intensity I_{15} (see Table 1):

$$\sigma_v = I_{15}\left(0.75 \cdot v_{hub} + 5.6\,\mathrm{m/s}\right) \tag{2}$$

This is not recommended for OWT, except for the design of the rotor and nacelle assembly [1]. For the support structure, the offshore turbulence intensity is described based on an approximation of the 90th percentile of the standard deviation of the horizontal wind speed v_{hub} at hub height z_{hub} [1]:

$$\sigma_{v90} = \frac{v_{hub}}{ln\,(z_{hub}/z_0)} + 1.28 \cdot 1.44\,\mathrm{m/s} \cdot I_{15} \tag{3}$$

where z_0 is the surface roughness length and I_{15} is the average turbulence intensity at hub height at $15\,\mathrm{m/s}$ wind speed. The surface roughness length z_0 has to be solved iteratively with the following equation:

$$z_0 = \frac{A_C}{g} \left[\frac{\kappa \cdot v_{hub}}{ln\,(z_{hub}/z_0)} \right]^2 \tag{4}$$

where A_C is the Charnock parameter with $A_C = 0.011$ for open sea, $\kappa = 0.4$ is the von Karman parameter and g is the acceleration of gravity. Due to wind induced waves, the surface roughness increases with increasing wind speed. This leads again to a slight increase of the turbulence intensity for high wind speeds.

For a neutrally stratified atmosphere, the wind profile can be described by the so-called power law profile [1,4]:

$$v(z) = v_{hub} \left(\frac{z}{z_{hub}} \right)^\alpha \tag{5}$$

with the mean horizontal wind speed $v(z)$ at the height z above the ground, the mean horizontal wind speed v_{hub} at hub height z_{hub} and the wind shear exponent α. The IEC standards [1,4] recommend a wind shear exponent of 0.2 for onshore and 0.14 for offshore conditions, respectively.

2.2. Analysis of FINO 1 Measurements

In order to allow a comparison taking into account site-specific wind field parameters, the wind speed measurements of the FINO 1 offshore research platform are analyzed for the period between January 2004 and December 2010. The FINO 1 platform is located in the North Sea, 45 km north of the island Borkum and near the offshore wind farm Alpha Ventus. The platform is equipped with a met mast with a height of about 100 m and records the long term meteorological and oceanographic conditions [19]. The wind speed and wind directions are measured on different heights with cup anemometers, UltraSonic Anemometers (USA), and classic wind vanes. The position of the different sensors are shown in Figure 1. In the present study, 10 min mean wind data of the cup anemometers and the wind vanes are analyzed. The objective is to derive the wind field parameters which are necessary for the aeroelastic simulations. An extensive analysis of the wind conditions are given for example in [20–22] for the period between September 2003 and August 2007.

Figure 2 shows the measured wind speed distribution with a mean wind speed of $9.4\,\mathrm{m/s}$ and the wind direction distribution at 90 m height. The measured wind speed distribution can be fitted by means of a Weibull distribution. The resulting scale and shape parameters are $A = 10.62\,\mathrm{m/s}$ and $k = 2.17$, respectively.

Figure 1. FINO 1 offshore research platform in the North Sea with the different sensor positions [19].
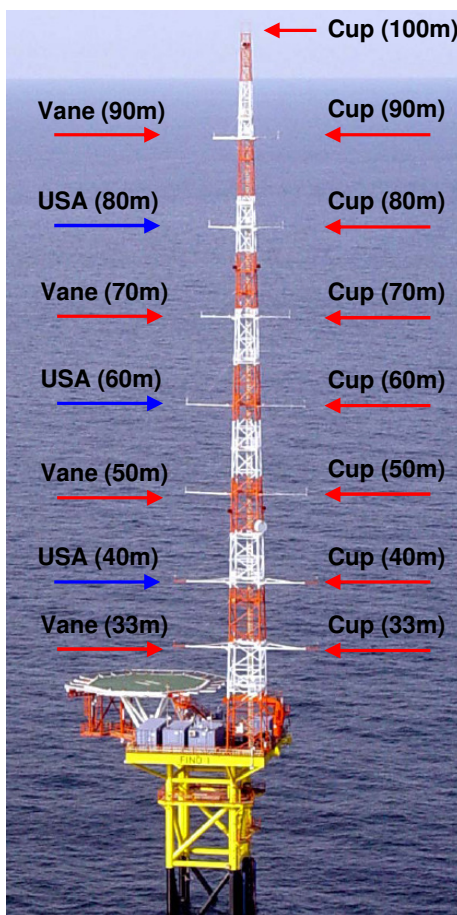
Figure 2. Distribution of wind speed and wind direction as measured at the FINO 1 platform from January 2004 to December 2010 at 90 m height. (**a**) Wind speed; (**b**) Wind direction.
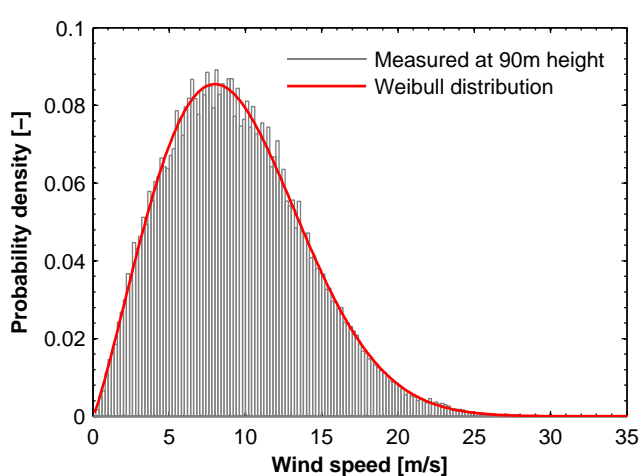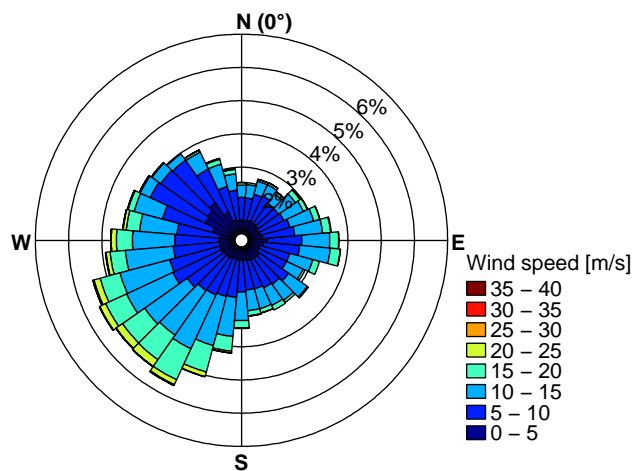
(a)   (b)

In the analysis it can be observed that the tower shadow of the met mast causes strong disturbances of the wind field for wind directions between 280° and 350°. This is also mentioned by Türk *et al.* [22]. For this reason, the wind sector 280°–350° is not further considered in the following investigations.

2.2.1. Turbulence Intensity

The turbulence intensity at the FINO 1 platform is determined by means of Equation 1 with the measured standard deviation and the mean wind speed of the cup anemometers. Due to wind direction fluctuations, the given standard deviation of the cup anemometers is not exactly the standard deviation of the horizontal wind speed, though close to it [22]. The scattering of the turbulence intensity depending on wind speed at 90 m height is shown in Figure 3.

Figure 3. Measured turbulence intensity depending on wind speed at FINO 1 at 90 m.
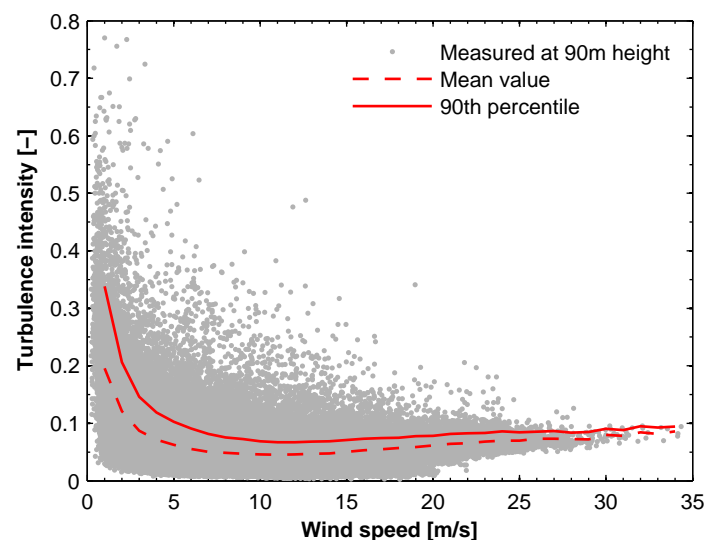
In the IEC standard 61400-3 [1] the 90th percentile turbulence intensity depending on wind speed is required as an input parameter for the load simulations. Therefore, the FINO 1 data is subdivided into 1 m/s wind speed bins for which the mean value and the 90th percentile are calculated (see Figure 3). Figure 4 shows the comparison of the measured 90th percentile turbulence intensity with 95% confidence intervals. The confidence intervals are estimated by using a bootstrap procedure with 5000 resamplings. In addition, the given relations in the IEC 61400-3 standard are shown. IEC C onshore denotes the normal turbulence model according to Equation 2 which can be used for the design of the rotor and nacelle assembly. For the design of the support structure, IEC C offshore denotes the turbulence conditions based on Equation 3. For both relations, a reference turbulence intensity $I_{15} = 0.12$ is used in accordance with the IEC standard (see Table 1). Except of wind speeds lower than 4 m/s, the measured turbulence intensities lie below the IEC C offshore values, and obviously, for all wind speeds they lie below the IEC C onshore values. To get a better matching between the FINO 1 turbulence intensities and the IEC C offshore values, for example [21,22] suggest a modification of Equation 3. Due to wind induced waves, which causes increasing surface roughness, the turbulence intensity increases again for high wind speeds. For the measured turbulence intensity this effect is stronger compared to the IEC C offshore values, while the normal turbulence model (IEC C onshore) does not consider this effect.

Figure 4. The 90th percentile of the measured turbulence intensity and mean value of the measured wind shear exponent depending on wind speed and in comparison to the IEC standard 61400-3 [1]. (**a**) Turbulence intensity; (**b**) Wind shear exponent.

(a)   (b)
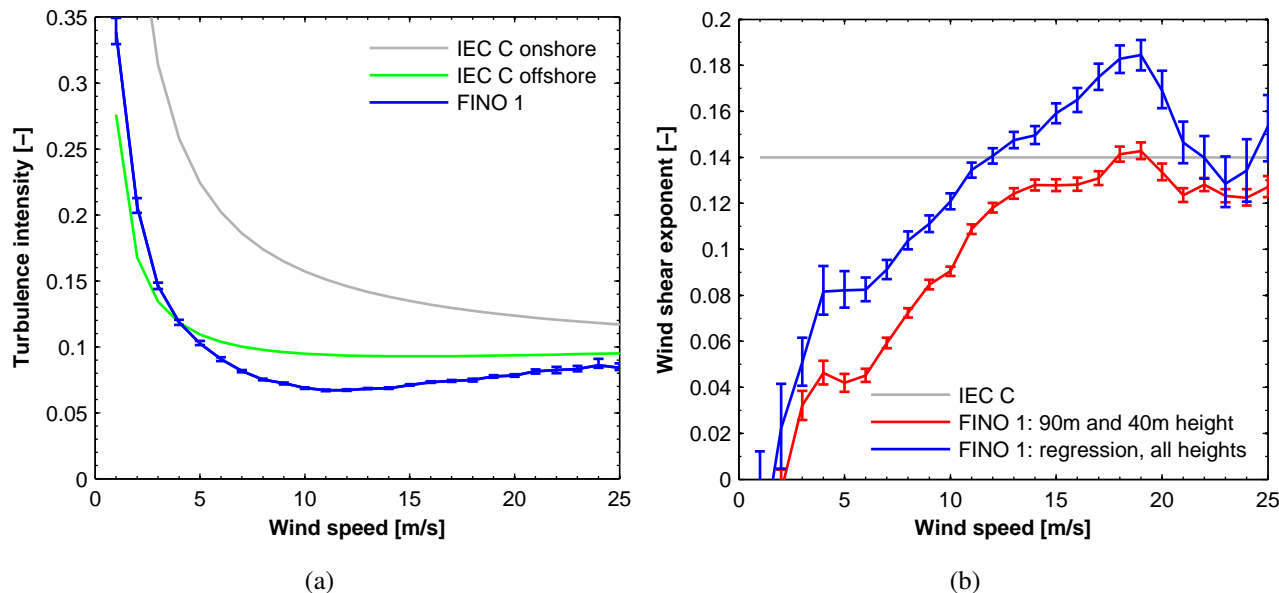
2.2.2. Wind Shear

The wind shear exponent α is determined by means of rearranging Equation 5. The mean horizontal wind speeds at 90 m and 40 m height are analyzed, because 90 m indicates the hub height of the wind turbine model and 40 m is near the lower end of the rotor plane. This results in a mean wind shear exponent of $\alpha = 0.09$, which is significantly lower than the recommended IEC-value of $\alpha = 0.14$ for offshore-sites [1]. In Figure 4, the mean values of the measured wind shear exponent based on the two heights are compared to the value given in the IEC 61400-3 standard. The measured wind shear exponent shows a strong dependence on the wind speed and atmospheric stability. Up to the 19 m/s wind speed bin, the measured wind shear exponent increases and is finally slightly higher than the IEC-value. Excluding these data, all other measured values are obviously lower. Especially at low wind speeds, very low wind shear exponents are observed. This reflects unstable atmospheric conditions with a well-mixed boundary layer, which leads to very small vertical wind speed gradients [20]. These results are very sensitive to wind speed fluctuations in one of the two heights. In order to estimate more robust wind shear exponents, a nonlinear regression over all cup anemometers from 33 m to 100 m height is performed. The hub height of the wind turbine model $z_{hub} = 90$ m is the reference height and for the regression a Levenberg–Marquardt algorithm is used. This yields a higher mean wind shear exponent $\alpha = 0.138$ but with a similar characteristic dependence on wind speed compared to the previous analysis. The mean wind shear exponents, based on the regression over all heights, are also shown in Figure 4. The error bars indicate the 95% confidence intervals, which are also estimated by means of a bootstrap procedure with 5000 resamplings. Due to inconsistent datasets over all heights, the number of available datasets for the regression is significantly lower than the number of datasets based on only two heights. Therefore, the uncertainties of the mean wind shear exponents based on the regression over all heights are higher compared to the exponents based on 90 m and 40 m height.

3. Simulations

Based on the comparison of the wind field parameters, aeroelastic simulations will be performed in order to investigate the effects of the loads on the OWT structure. For the investigations, the aeroelastic model of a 5 MW OWT with a rotor diameter of 126 m and a hub height of 90 m is used [23]. The OWT is pitch regulated and operates with variable speed. The rated wind speed is 11.4 m/s and the maximum rotor speed is 12.1 rpm. The OWT model was developed at the National Renewable Energy Laboratory (NREL) with different platform configurations. In order to simplify the model, wave loads are not considered in this study and therefore the land-based tower model is used. The aeroelastic simulations are performed with the simulation software FAST [24]. The wind fields are generated with TurbSim [25] on a 31×31 square grid with 145 m width, which is centered at the hub height of the wind turbine model. Detailed turbulence data at FINO 1 were not available in the present study, therefore the Kaimal turbulence spectrum is used. Between the cut-in wind speed $v_{in} = 3 \,\text{m/s}$ and the cut-out wind speed $v_{out} = 25 \,\text{m/s}$, wind fields with 12 different mean wind speeds are generated (3 m/s, 5 m/s,..., 25 m/s). The generated wind fields are based on the turbulence intensities and wind shear exponents shown in Figure 4. For the IEC C onshore and IEC C offshore inputs, two different turbulence intensity characteristics and a constant wind shear exponent of $\alpha = 0.14$ are used, while for the FINO 1 inputs the wind shear exponent depends on wind speed. There are two different variations based on the analysis of the FINO 1 data in the previous section. Below, FINO 1 V1 denotes the simulations with the wind shear exponents derived from the heights 90 m and 40 m. The simulations with the regression-based wind shear exponents are denoted as FINO 1 V2. In both cases the 90th percentiles of the measured turbulence intensities at the FINO 1 platform are used as input parameters (Figure 4).

The flapwise and edgewise bending moments at the blade root are then analyzed in terms of fatigue and extreme loads. The load extrapolation methods used require a large amount of various simulations. According to the IEC standard 61400-1 [4], at least 15 simulations with 10 min duration are required for wind speeds above the rated wind speed of the wind turbine. Based on the results of Fogle *et al*. [7] and Moriarty *et al*. [9], for each input configuration (mean wind speed, turbulence intensity, wind shear exponent), 30 simulations are performed with 10 min duration and different random seeds. For each simulation the random seeds are randomly chosen within the range which is given in TurbSim. In total, this results in 1440 ($= 4 \cdot 12 \cdot 30$) simulations. Furthermore, load extrapolation methods require wind speed distributions to calculate the long-term distributions of loads. For both IEC cases, the wind speed is assumed to be Rayleigh distributed with 10 m/s mean wind speed. As already mentioned above, at the FINO 1 platform the wind speed is Weibull distributed.

3.1. Fatigue Loads

The fatigue loads are analyzed by means of the damage-equivalent load-range approach. For the time series, rainflow counting is used to determine the amplitudes R_i and the corresponding number of load cycles n_i. Based on the IEC standard 61400-13 [26], the damage-equivalent load is defined as

$$R_{eq} = \left(\frac{\sum_i R_i^m \cdot n_i}{n_{eq}} \right)^{1/m} \tag{6}$$

where m is the Wöhler curve exponent and n_{eq} is the equivalent number of load cycles. The damage-equivalent flapwise and edgewise bending moments at the blade root are calculated with $m = 10$ and $n_{eq} = 600$ for each 10 min time series. This results in an equivalent frequency of 1 Hz. Figure 5 shows the mean values of the damage-equivalent flapwise and edgewise bending moments of 30 simulations. As might be expected, due to the highest turbulence intensities the IEC C onshore conditions yield the largest damage-equivalent loads. Except when the mean wind speed is lower than 5 m/s, the IEC C offshore conditions also yield larger loads than the simulations based on the FINO 1 data. The differences of the loads between the IEC C onshore and the IEC C offshore simulations are significantly larger than the differences between the FINO 1 V1 and V2 loads. The IEC wind fields differ in terms of their turbulence intensities. In contrast to that, the FINO 1 wind fields differ in terms of their wind shear exponents. Therefore, the damage-equivalent flapwise and edgewise bending moments are more affected by the turbulence intensity than by the wind shear exponent. The main differences of the loads between both FINO 1 variations correspond to the main differences of the wind shear exponent in the wind speed range from 15 m/s to 19 m/s (see Figures 4 and 5). These differences are about 8.5% for the flapwise bending moment and 0.5% for the edgewise bending moment. Near the rated wind speed of 11.4 m/s the equivalent flapwise bending moment of the IEC C onshore and IEC C offshore conditions are 25% to 80% higher compared with the FINO 1 conditions. These significant differences are caused by the about two times higher turbulence intensities of the IEC C onshore condition compared with the FINO 1 conditions. The higher turbulence intensity leads to a larger range of wind speed fluctuations within a 10 min simulation, which require additional pitch control motions and result in higher amplitudes of the flapwise bending moment. For the maximum equivalent flapwise bending moments at 25 m/s, this increase is between 2% and 26%. The edgewise bending moments are only up to 8% higher because these are mainly caused by gravity forces and less affected by turbulence intensity or wind shear.

Figure 5. Mean value of the damage-equivalent bending moments at the blade root. (**a**) Flapwise; (**b**) Edgewise.

(a)

(b)
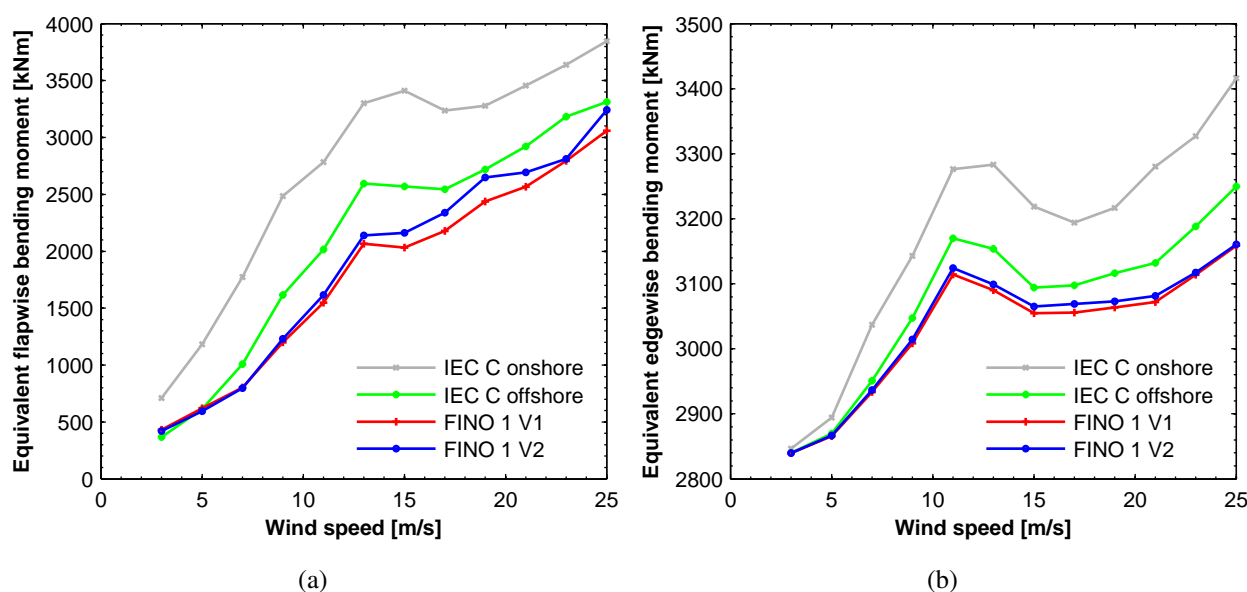
3.2. Extreme Loads

3.2.1. Peak Over Threshold Extrapolation Method

In case of a peak extrapolation method, there are three different ways to extract peaks from 10 min time series: global maxima, block maxima, and peak over threshold. If global maxima is used, only the largest peak within a 10 min time series is extracted. For block maxima, the time series are divided into equally distributed time blocks and from each block the largest peak is extracted. The Peak Over Threshold (POT) method extracts several peaks in every 10 min time series. Thereby, the largest value between each successive upcrossing of the threshold is extracted. Investigations have shown that the POT method yields superior results in comparison to the other methods [11,12]. In the literature and in the IEC standard it is recommended to choose a threshold which is the mean value plus 1.4 times the standard deviation ($\mu + 1.4\sigma$) [4,9]. Moreover, determining an optimal threshold can lead to better fits of the distributions [11]. The aggregation of the peaks at each individual mean wind speed can be done by means of two procedures "fitting before aggregation" or "aggregation before fitting". Toft *et al.* [12] showed that the "fitting before aggregation" approach yields the best results. For the extracted and aggregated peaks, local distribution functions have to be fitted for each given mean wind speed v. In the literature, several distribution functions are used: three parameter Weibull (W3P), Weibull, normal, Rayleigh, Gumbel, *etc.* However, in general a W3P distribution function is preferred for the local distributions [5,11,12,27]:

$$F_{local}(x \mid \tau, v) = 1 - \exp\left(-\left(\frac{x - \gamma}{\beta}\right)^{\alpha}\right) \tag{7}$$

where x is the considered load of the OWT and τ is the length of each time series. Based on the local distribution, the short-term distribution for the maximum load within a time series of the length τ is given as

$$F_{short-term}(x, \tau, v) = F_{local}(x \mid \tau, v)^{n(v,\tau)} \tag{8}$$

where $n(v, \tau)$ is the average number of independent peaks at the mean wind speed v within the time interval $[0, \tau]$. Then, the long-term distribution can be approximately determined by integrating over the mean wind speeds given by the density function $f_v(v)$:

$$F_{long-term}(x \mid \tau) = \int_{v_{in}}^{v_{out}} F_{short-term}(x \mid \tau, v) f_v(v) \mathrm{d}v \tag{9}$$

Furthermore, it is assumed that $f_v(v)$ is truncated to the interval $[v_{in}, v_{out}]$ [12]. Under the assumption that the individual time series are independent, the probability for the characteristic extreme load x_c with a recurrence period of T_c (years) is then defined as

$$F_{long-term}(x_c \mid \tau) = 1 - \frac{\tau}{60 \cdot 24 \cdot 365 \cdot T_c} \tag{10}$$

The method considered in the present paper can be summarized as follows: POT extraction with a threshold $\mu + 1.4\sigma$, "aggregation before fitting" and a W3P distribution to fit the local distributions. In order to ensure that the extracted peaks are independent, the independency is tested by Blum's test [28],

which is also used by Fogle *et al.* [7]. Blum's test uses a test statistic B that has to be lower than a critical value B_{cr}. For a significance level of 1% the critical value is $B_{cr} = 4.23$. For the different input configurations, the mean B values are estimated for each wind speed bin. The values of the flapwise bending moment are lower than $B = 3.5$, which is also lower than the critical value. In addition, the sample correlation coefficients ρ are determined. It turns out that all coefficients are lower than $\rho = 0.24$. Therefore, independency of the extracted flapwise bending moments can be assumed. In terms of the edgewise bending moment, bins with a low wind speed have mean B values up to $B = 16$ while for higher wind speeds the mean values are also significantly lower than the critical value. The sample correlation coefficients show a similar characteristic, with correlation coefficients up to $\rho = 0.67$ for bins with a low wind speed and less than $\rho = 0.2$ for high wind speeds. For high wind speeds, it can be assumed that the extracted edgewise bending moments are independent. The independency of the extracted edgewise bending moments at low wind speeds could be improved by adding a minimum separation time between the peaks. According to Ragan and Manuel [11], the requirement of a minimum separation time between the extracted peaks only has a small effect on the extrapolated long-term load predictions. Moreover, it would significantly reduce the amount of available data and the procedure would be more complicated. Due to this and due to the reason that the peak loads at low wind speeds have only a small effect on the extrapolated loads, no separation time is used. As already mentioned above, 30 time series of 10 min duration are available for each input configuration.

Figure 6. Long-term exceedance probability distribution of the bending moments at the blade root calculated by means of the POT method. (**a**) Flapwise; (**b**) Edgewise.

(a)　　　　　　　　　　　　　　　　　　　　　　　　　　　　　(b)
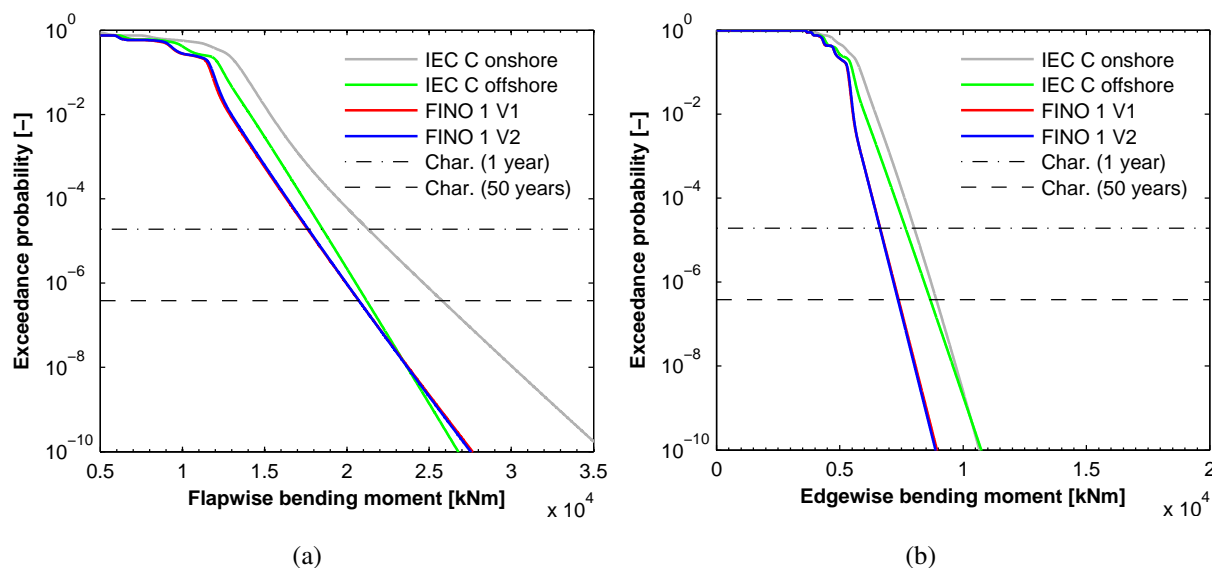
Figure 6 shows the resulting long-term exceedance probability distributions of the flapwise and edgewise bending moments at the blade root. In addition to this, Table 2 shows the characteristic extreme loads with a recurrence period of 1 year and 50 years. There are almost no differences between the characteristic extreme loads of FINO 1 V1 and V2. Therefore, the extreme loads are also more affected by the turbulence intensity than the wind shear. In comparison to the characteristic extreme flapwise bending moment (50 years recurrence period) of the FINO 1 data, the IEC C offshore value is 2% higher

and the IEC C onshore value is 24% higher. In terms of the edgewise bending moment, the increases are about 17% and 21%, respectively. Typically, the edgewise bending moments are mainly dominated by gravity forces, so that such a high increase could not be expected. The fits of the local distribution functions based on the IEC C simulations are worse compared to the FINO 1 data. Especially, for the wind speed $v = 13\,\mathrm{m/s}$ the local distribution function significantly overestimates the tail of the extracted edgewise bending moments of the IEC C simulations (Figure 10). This leads also to an overestimation of the characteristic extreme edgewise bending moment and therefore to a large difference between IEC C and FINO 1 results.

Table 2. Characteristic extreme loads calculated by means of the POT method.

	Flapwise bending moment [kNm]		Edgewise bending moment [kNm]	
Characteristic	**1 year**	**50 years**	**1 year**	**50 years**
IEC C onshore	21,292	25,798	8,023	8,916
IEC C offshore	18,520	21,204	7,672	8,672
FINO 1 V1	17,607	20,735	6,643	7,386
FINO 1 V2	17,654	20,739	6,628	7,358

3.2.2. Average Conditional Exceedance Rates

A novel extrapolation method for predicting characteristic extreme loads with a certain recurrence period is based on Average Conditional Exceedance Rates (ACER). This method was developed by Naess and Gaidai [17,18] and was already applied to estimate extreme wind speeds [29] or to determine extreme loads of wind turbines [5]. In the following a short overview is given in terms of the estimation of empirical ACER functions. For the theoretical background it is referred to [5,17,18,29]. If M simulated time series of the length τ with N extracted peaks are available, the exceedance rate can be empirically estimated by counting the number of conditional exceedances of the load level η. The exceedance rate, which is conditioned on the $k-1$ previous non-exceedances, can be empirically estimated for each time series by [5]:

$$\hat{\varepsilon}_k^{(i)+}(\eta \mid Q, R) = \frac{1}{N} \sum_{j=k}^{N} A_{kj}^{(i)}(\eta \mid Q, R) \quad \text{for} \quad i = 1, ..., M \tag{11}$$

The variables Q and R describe an ergodic process and a time-invariant non-ergodic field, respectively. Furthermore, A_{kj} is a random function

$$A_{kj} = \mathbf{1}\left\{Y_j > \eta, Y_{j-1} \leq \eta, ..., Y_{j-k+1} \leq \eta\right\} \tag{12}$$

for $j = k, ..., N$ and $k = 2, 3, ...$, where Y_j denotes the peak value of the load series at a certain time and $\mathbf{1}\{\mathcal{A}\}$ is the indicator function of a random process $\mathcal{A}$. Based on the empirically estimated exceedance rate (Equation 11), the ACER function for M simulations is given by:

$$\hat{\varepsilon}_k^+(\eta \mid Q, R) = \frac{1}{M} \sum_{i=1}^{M} \hat{\varepsilon}_k^{(i)+}(\eta \mid Q, R) \tag{13}$$

In order to approximate the empirically estimated ACER function, an appropriate asymptotic extreme value distribution of the Gumbel type with four parameters is used [5]:

$$\hat{\varepsilon}_k^+(\eta \mid Q, R) = q(\eta) \exp(-a(\eta - b)^2), \quad \eta \geq \eta_0 \tag{14}$$

To reach better fits of the ACER function, a tail marker η_0 is introduced, because exceedance rates at small load levels η are not very representative for the extreme value distribution. The optimal values of the parameters a, b, c and q can be determined by minimizing the following mean square error function [5,18,29]:

$$\sum_{j=1}^{L} w_j \left[\log \hat{\varepsilon}_k^+(\eta_j \mid Q, R) - \log q + a(\eta_j - b)^c\right]^2 \tag{15}$$

where L is the number of considered load levels and w_j is a weight factor based on the 95% confidence interval CI of the empirically estimated ACER function, which puts more emphasis on the more reliable data points with a low level of uncertainty:

$$w_j = \frac{1}{\left[\log CI^+(\eta_j \mid Q, R) - \log CI^-(\eta_j \mid Q, R)\right]^2} \tag{16}$$

Based on Equation 16, load levels with small relative confidence intervals of the empirically estimated ACER function get higher weight factors. As described in [5,18,29], the minimization of Equation 15 can be done by using the Levenberg–Marquardt least square optimization method. The success of this optimization highly depends on the chosen start values of the individual parameters. A procedure to define reasonable initial guesses is presented for example in [5].

In the present study, the only ergodic variable in Q is the mean wind speed v. Due to reasons of simplicity, the time-invariant non-ergodic variables R, which represent the model and statistical uncertainty, are not taken into account [5]. Then, the reduced distribution function for the long-term extreme loads $\hat{X}(\mathcal{T})$ is given as

$$F_{\hat{X}(\mathcal{T})}^{(k)}(\eta) = \exp\left(-n\mathbb{E}_v\left[\varepsilon_k^+(\eta \mid v)N(v)\right]\right) \tag{17}$$

The expected value with respect to the mean wind speed v can be determined by

$$\mathbb{E}_v\left[\varepsilon_k^+(\eta \mid v)N(v)\right] = \int_{v_{in}}^{v_{out}} \varepsilon_k^+(\eta \mid v)N(v)f_v(v)\mathrm{d}v \tag{18}$$

In the present study, the expected value is calculated numerically based on 12 different mean wind speeds. For each wind speed 30 time series with 10 min duration are used, where each is divided into 20 time intervals with the same length. Then, the maximum peak in each interval is extracted. The

results of Toft *et al.* [5] show that there are only small differences between the unconditional ACER (ε_1^+) and conditional ACER functions (ε_k^+; $k \geq 2$) for the tail values. Because of this, only unconditional exceedance rates (ε_1^+) are used in the following. In order to fit the ACER function, the tail marker is chosen by means of a simple optimization. In only a few cases the optimization performs poorly. Then, the tail marker is defined manually in the way that the remaining data is sufficient for the fit.

Figure 7 shows the resulting long-term exceedance probability distributions of the flapwise and edgewise bending moments at the blade root. Furthermore, in Table 3 the corresponding characteristic extreme loads are presented with a recurrence period of 1 year and 50 years, respectively. Corresponding to the results of the POT methods, almost no differences can be identified between the characteristic extreme loads of FINO 1 V1 and V2. Compared to the data based on FINO 1, the characteristic flapwise bending moments (50 years recurrence period) of the IEC standard conditions are 15% to 30% higher. The characteristic edgewise bending moments of FINO 1 and IEC C offshore are nearly identical. Compared with that, the characteristic edgewise bending moment of IEC C onshore is about 12% higher.

Figure 7. Long-term exceedance probability distribution of the bending moments at the blade root calculated by means of the ACER method. (**a**) Flapwise; (**b**) Edgewise.

(a)   (b)
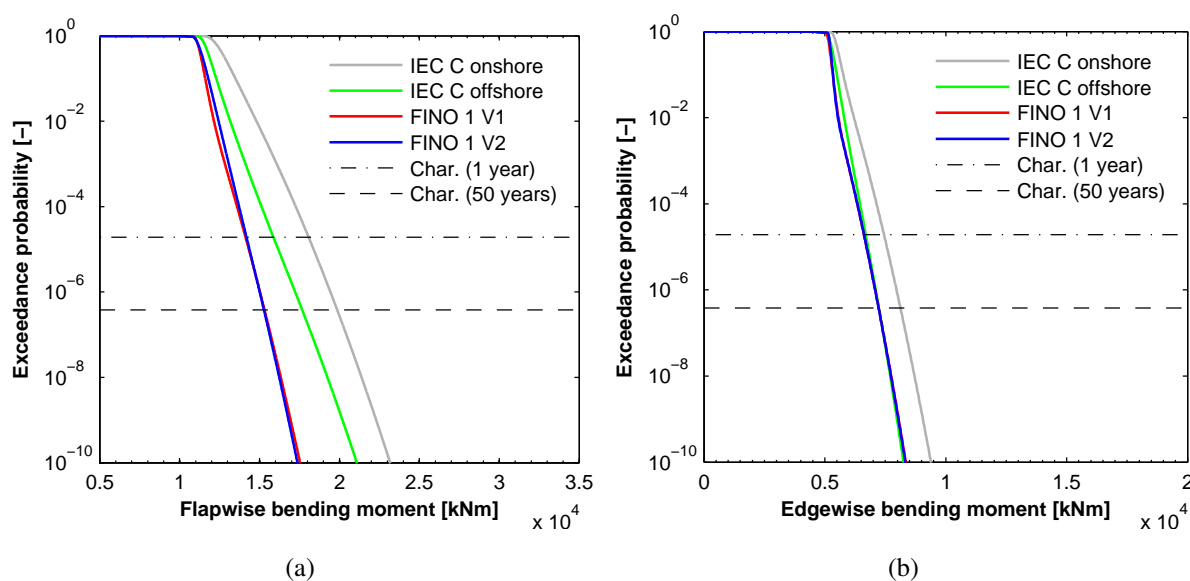
Table 3. Characteristic extreme loads calculated by means of the ACER method.

Characteristic	Flapwise bending moment [kNm]		Edgewise bending moment [kNm]	
	1 year	**50 years**	**1 year**	**50 years**
IEC C onshore	18,078	19,861	7,447	8,126
IEC C offshore	15,876	17,669	6,692	7,234
FINO 1 V1	14,129	15,313	6,617	7,227
FINO 1 V2	14,189	15,276	6,619	7,223

3.2.3. Convergence Criteria

As mentioned above, based on the results of Fogle *et al.* [7] and Moriarty *et al.* [9], for each input configuration (mean wind speed, turbulence intensity, wind shear exponent) 30 simulations are performed. In general it can be stated that more simulations lead to a larger number of extracted peaks, which can help to get a better fit for the tail of the short-term distributions. This will reduce the uncertainty of the aggregated long-term distribution and also of the extrapolated extreme loads [7]. In order to show that 30 simulations for each input configuration are sufficient and an acceptable uncertainty level is reached, a convergence criterion in form of a normalized confidence interval is used:

$$\frac{\hat{L}_{\alpha,p} - \hat{L}_{(1-\alpha),p}}{\hat{L}_p} < \frac{q}{100} \tag{19}$$

where the denominator $\hat{L}_p$ represents the p-quantile load of the empirical short-term load distribution and the numerator represents the $(2\alpha - 1)\%$ confidence interval on the p-quantile load. The variable q describes the maximum acceptable percentage error permitted on the normalized confidence interval [7]. In the IEC standard 61400-1 [4] q is 15%, and in case of global maxima, the normalized 90% confidence interval on the 84th-quantile load is considered. If more load peaks are extracted within a 10 min time series by means of the block maxima or the POT method, the p-quantile with

$$p = 0.84^{\frac{1}{n(v)}} \tag{20}$$

must be chosen, where $n(v)$ is the average number of independent peaks at the mean wind speed v within the 10 min time interval. In the IEC standard [4], the bootstrap method is one of the recommended methods to estimate the confidence interval on the p-quantile load. Based on the original sample (extracted load peaks), the bootstrap method creates a large number of random resamplings with replacement which have the same size as the original sample. The p-quantile can be determined for each newly created sample and based on these the confidence interval can be estimated. An extensive description of the bootstrap method is given in [30]. In the present study, 5000 resamplings are used to estimate the 90% confidence intervals on the p-quantile loads. The bootstrap method is based on a random process, therefore the bootstrap simulation is repeated 10 times for each mean wind speed. Figure 8 shows the mean values of the normalized 90% confidence intervals on the p-quantile of the flapwise bending moments for the POT and ACER method.

Figure 8. Normalized 90% confidence interval on the p-quantile of the flapwise bending moment based on (**a**) POT; (**b**) ACER method.

(a)

(b)
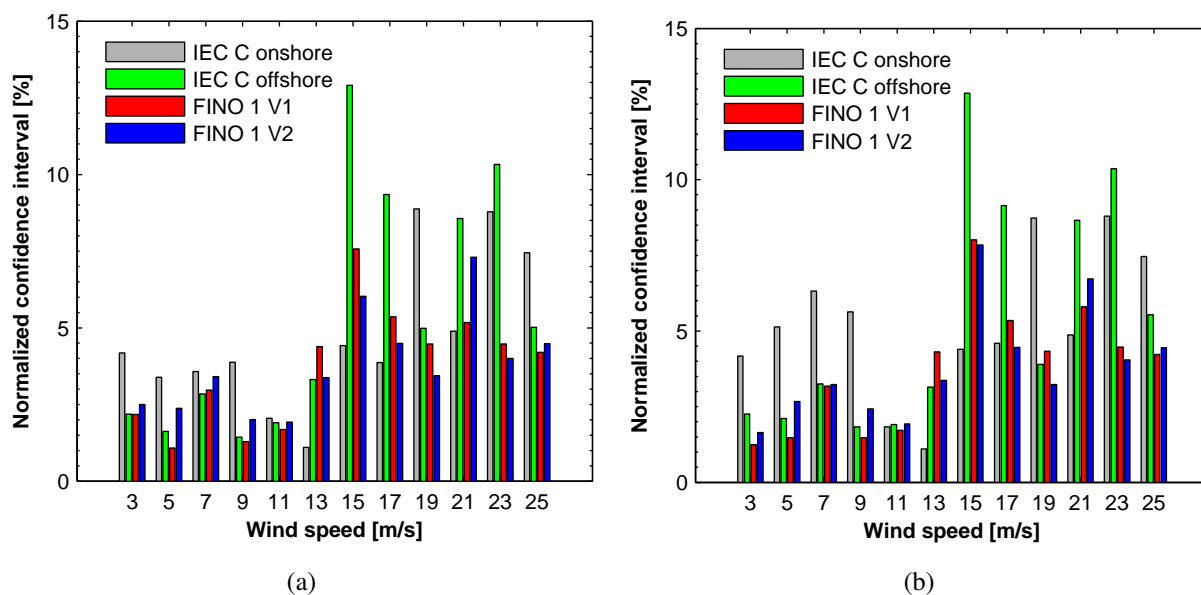
For all wind speeds, the mean values of the confidence interval are lower than 15%. Due to a low standard deviation in all cases, the maximum value of the confidence interval is also lower than 15%. The normalized confidence intervals of the edgewise bending moments are lower than 10%. Thus, it can be assumed that 30 simulations are sufficient in the present study.

3.2.4. Comparison

The results of the POT method and the ACER method (Tables 2 and 3) show that the characteristic extreme loads obtained by the POT method are generally larger. Furthermore, the characteristic of the long-term exceedance distributions differ significantly (compare Figures 6 and 7). In comparison to the ACER method, an increase of the flapwise bending moment leads to minor changes in the exceedance probability based on the POT method. Reasons for this are the differences of the POT and ACER method itself as well as the different distribution functions used. The three parameter Weibull distribution is generally preferred in literature for the POT method and also yields consistently good results in the present study. According to [5], the Gumbel distribution is used for the ACER method. In Figure 9, it is shown that the data fits of the POT method are worse compared with fits of the ACER method. Except for the wind speed $v = 13\,\mathrm{m/s}$, the empirical ACER functions are fitted very well. In contrast to that, the local distribution functions overestimate the tail of the extracted data based on the POT method. In Figure 10, this is also seen for the local distributions of the edgewise bending moments. Therefore, it is assumed that the characteristic loads obtained by means of the ACER method are more plausible.

Figure 9. Local exceedance probability distribution for the flapwise bending moment at the blade root (please notice the different scales of the y-axis). (**a**) POT, $v = 11m/s$; (**b**) ACER, $v = 11m/s$; (**c**) POT, $v = 13m/s$; (**d**) ACER, $v = 13m/s$; (**e**) POT, $v = 21m/s$; (**f**) ACER, $v = 21m/s$.

(a)

(b)

(c)

(d)

(e)

(f)
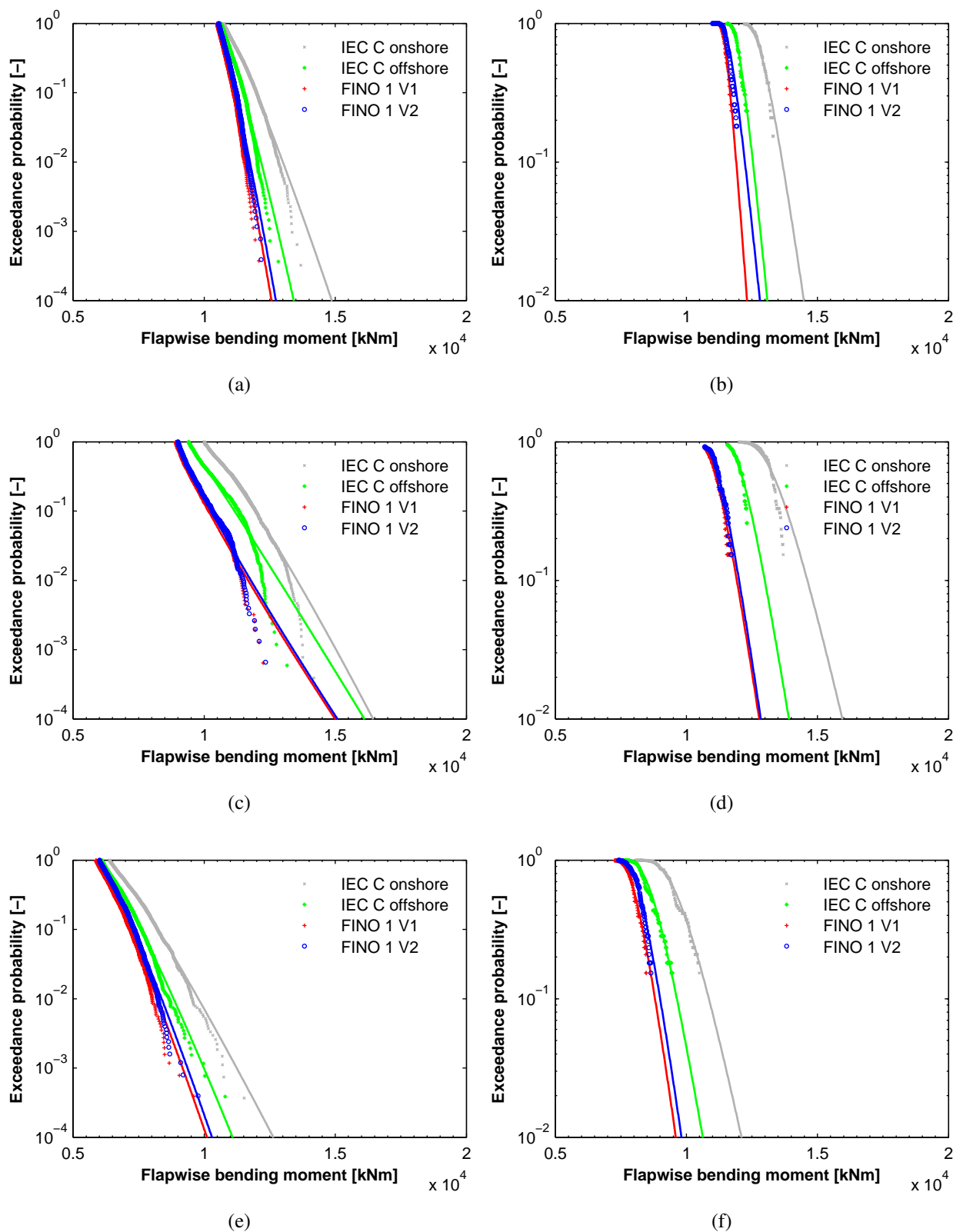
Figure 10. Local exceedance probability distribution for the edgewise bending moment at the blade root (please notice the different scales of the y-axis). (**a**) POT, $v = 11m/s$; (**b**) ACER, $v = 11m/s$; (**c**) POT, $v = 13m/s$; (**d**) ACER, $v = 13m/s$; (**e**) POT, $v = 21m/s$; (**f**) ACER, $v = 21m/s$.
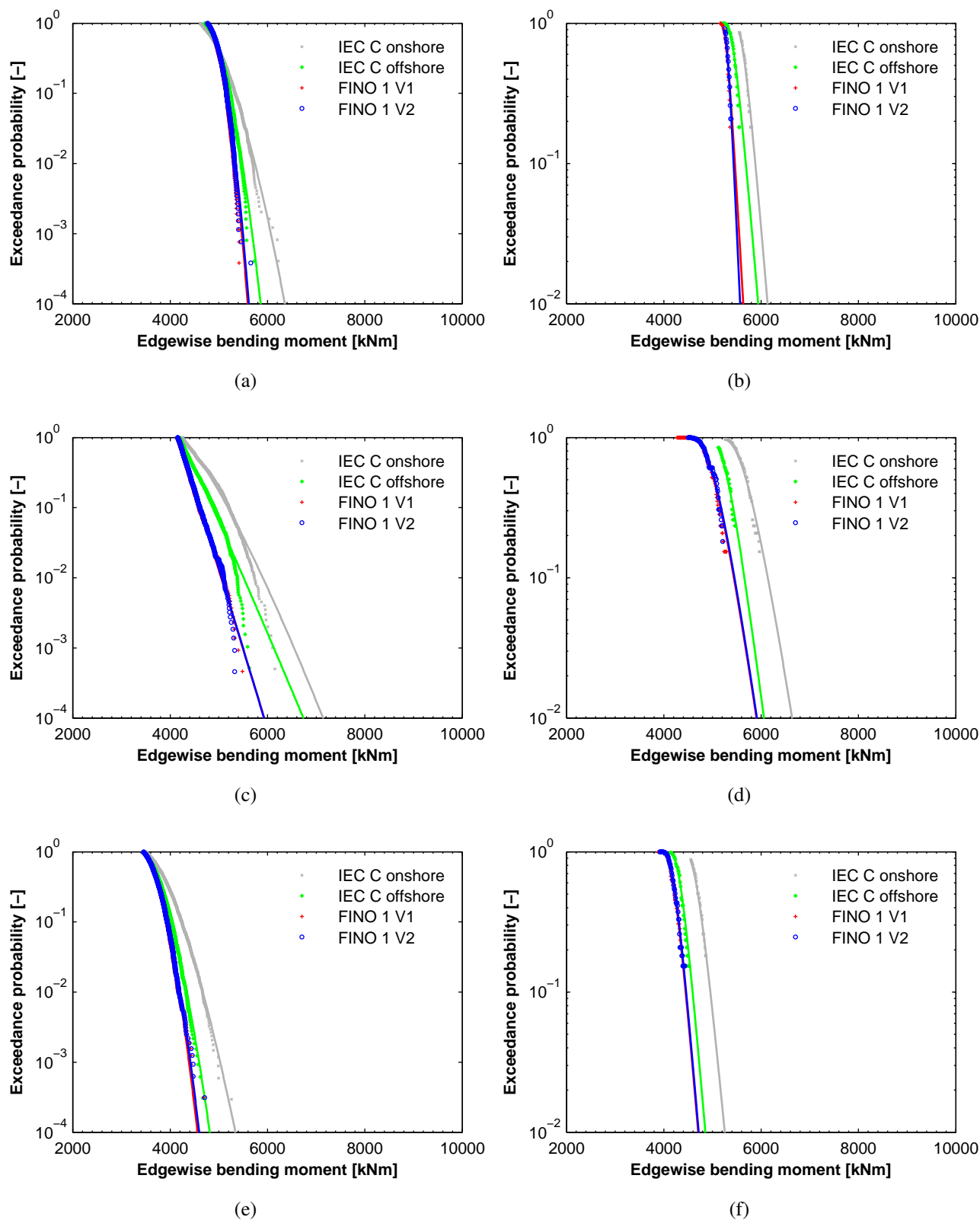
4. Conclusions

The wind speed measurements of the FINO 1 offshore research platform are analyzed based on the 10 min mean wind data of the cup anemometers. The 90th percentile of the turbulence intensity is determined at 90 m height. Except when the wind speed is low, the measured turbulence intensities are lower compared with the values in the IEC standard. The wind shear exponent is determined in two different ways. On the one hand, only the heights 90 m and 40 m are considered, and on the other hand a regression is performed over all cup anemometers on the different heights at FINO 1. Both methods show a similar characteristic depending on wind speed, but the regression-based wind shear exponents are significantly higher, which reflect more stable atmospheric conditions. Based on this analysis, aeroelastic simulations are performed, and the resulting fatigue and extreme loads of a 5 MW wind turbine model are investigated.

The fatigue loads are determined by means of the damage-equivalent load-range approach. The largest damage-equivalent flapwise bending moment based on the IEC standard is up to 26% higher than the corresponding results for the FINO 1 data. The largest damage-equivalent edgewise bending moment is only up to 8% higher because edgewise bending moments are mainly caused by gravity forces and thus less affected by turbulence intensity.

In order to determine the extreme loads with a recurrence period of 50 years, a peak over threshold $(\mu + 1.4\sigma)$ extrapolation method and a recently developed method based on Average Conditional Exceedance Rates (ACER) are used. Depending on the extrapolation method, the characteristic flapwise bending moment based on the design requirements of the rotor and nacelle assembly in the IEC standard is 24% to 30% higher compared with the results based on the FINO 1 conditions. A comparison of the local distribution functions has shown that the results obtained by the ACER method are more plausible. For both methods, it is shown that 30 simulations reach a sufficient uncertainty level. However, further simulations could be performed to reduce the effects of the statistical uncertainty.

In summary, the fatigue and extreme loads are more affected by the turbulence intensity than by the wind shear exponent. For this reason, the requirements in the IEC standard 61400-3 are very conservative for the design of the rotor blades. It is shown that the simulations based on the requirements for the design of the support structure and also based on the site-specific wind field parameters yield significantly lower loads during power production. Therefore, the use of wind field parameters based on the requirements for designing the support structure or site-specific parameters could provide a large optimization potential to reduce weight and cost of the rotor blades. Besides the turbulence intensity and the wind shear exponent, there are also other factors influencing the calculated fatigue and extreme loads. These are for example measurement uncertainties, yawed inflow, the used turbulence spectrum, or the wind turbine control system. The simulations based on the FINO 1 data use only the measured 90th percentiles of the turbulence intensities at hub height and the measured wind shear exponents as input parameters. The Kaimal turbulence spectrum is used for all simulations. This model contain assumptions (e.g., invariant spectra across the grid or Gaussian statistics) that are not generally observed in measurements. In future work, the turbulence characteristic at the FINO 1 site should be investigated in more detail in order to generate more realistic wind fields and to determine their effects on the loads. Furthermore, also other design load cases have to be taken into consideration.

Acknowledgments

References

1. *International Electrotechnical Committee IEC 61400-3: Wind Turbines Part 3: Design Requirements for Offshore Wind Turbines*; 1st ed.; IEC: Geneva, Switzerland, 2009.

2. Veldkamp, D. Chances in Wind Energy—A Probabilistic Approach to Wind Turbine Fatigue Design. Ph.D. Dissertation, Wind Energy Research Institute, Delft University of Technology, Delft, The Netherlands, 2006.

3. Sørensen, J.D.; Toft, H.S. Probabilistic Design of Wind Turbines. *Energies* **2010**, *3*, 241–257.

4. *International Electrotechnical Committee IEC 61400-1: Wind turbines Part 1: Design Requirements*; 3rd ed.; IEC: Geneva, Switzerland, 2005.

5. Toft, H.S.; Naess, A.; Saha, N.; Sørensen, J.D. Response Load Extrapolation for Wind Turbines During Operation Based on Average Conditional Exceedance Rates. *Wind Energy* **2011**, *14*, doi: 10.1002/we.455.

6. Agarwal, P.; Manuel, L. Load Extrapolation Methods for Offshore Wind Turbines. In *Proceedings of Offshore Technology Conference*, Houston, TX, USA, 3–6 May 2010.

7. Fogle, J.; Agarwal, P.; Manuel, L. Towards an Improved Understanding of Statistical Extrapolation for Wind Turbine Extreme Loads. *Wind Energy* **2008**, *11*, 613–635.

8. Freudenreich, K.; Argyriadis, K. Wind Turbine Load Level Based on Extrapolation and Simplified Methods. *Wind Energy* **2010**, *11*, 589–600.

9. Moriarty, P.J.; Holley, W.E.; Butterfield, S.P. *Extrapolation of Extreme and Fatigue Loads Using Probabilistic Methods*; Report No. TP-500-34421; National Renewable Energy Laboratory: Golden, CO, USA, 2004.

10. Natarajan, A.; Holley, W.E. Statistical Extreme Load Extrapolation With Quadratic Distortions for Wind Turbines. *J. Sol. Energy Eng.* **2008**, *130*, 031017.

11. Ragan, P.; Manuel, L. Statistical Extrapolation Methods for Estimating Wind Turbine Extreme Loads. *J. Sol. Energy Eng.* **2008**, *130*, 031011.

12. Toft, H.S.; Sørensen, J.D.; Veldkamp, D. Assessment of Load Extrapolation Methods for Wind Turbines. *J. Sol. Energy Eng.* **2011**, *133*, 021001.

13. Cheng, P.W.; van Bussel, G.J.W.; van Kuik, G.A.M.; Vugts, J.H. Reliability-Based Design Methods to Determine the Extreme Response Distribution of Offshore Wind Turbines. *Wind Energy* **2003**, *6*, 1–22.

14. Saranyasoontorn, K.; Manuel, L. Efficient Models for Wind Turbine Extreme Loads Using Inverse Reliability. *J. Wind Eng. Ind. Aerodyn.* **2004**, *92*, 789–804.

15. Agarwal, P.; Manuel, L. Simulation of Wind Turbine Response for Long-Term Extreme Load Prediction. *Eng. Struct.* **2009**, *31*, 2236–2246.

16. Saranyasoontorn, K.; Manuel, L. Design Loads for Wind Turbines Using the Environmental Contour Method. *J. Sol. Energy Eng.* **2006**, *128*, 554–561.

17. Naess, A.; Gaidai, O. Monte Carlo Methods for Estimating the Extreme Response of Dynamical Systems. *J. Eng. Mech.* **2008**, *134*, 628–636.

18. Naess, A.; Gaidai, O. Estimation of extreme values from sampled time series. *Struct. Saf.* **2009**, *31*, 325–334.

19. Neumann, T.; Nolopp, K.; Strack, M.; Mellinghoff, H.; Söker, H.; Mittelstaedt, E.; Gerasch, W.J.; Fischer, G. Erection of German Offshore Measuring Platform in the North Sea. *DEWI Magazin* **2003**, *23*, 32–46.

20. Türk, M.; Grigutsch, K.; Emeis, S. The Wind Profile Above the Sea—Investigations Basing on Four Years of FINO 1 Data. *DEWI Magazin* **2008**, *33*, 12–16.

21. Türk, M. Ermittlung designrelevanter Belastungsparameter für Offshore—Windkraftanlagen. Ph.D. Disseration, Universität Köln, Cologne, Germany, 2008.

22. Türk, M.; Emeis, S. The dependence of offshore turbulence intensity on wind speed. *J. Wind Eng. Ind. Aerodyn.* **2010**, *98*, 466–471.

23. Jonkman, J.; Butterfield, S.; Musial, W.; Scott, G. *Definition of a 5-MW Reference Wind Turbine for Offshore System Development*; National Renewable Energy Laboratory: Golden, CO, USA, 2009; NREL/TP-500-38060.

24. Jonkman, J.M.; Buhl, M.J., Jr. *FAST User's Guide*; National Renewable Energy Laboratory: Golden, CO, USA, 2005; NREL/TP-500-38230.

25. Jonkman, B.J. *TurbSim User's Guide*; Version 1.50; National Renewable Energy Laboratory: Golden, CO, USA, 2009; NREL/TP-500-46198.

26. *International Electrotechnical Committee IEC TS 61400-13: Wind Turbine Generator Systems— Part 13: Measurement of Mechanical Loads*; 1st ed.; IEC: Geneva, Switzerland, 2001.

27. Moriarty, P.J.; Holley, W.E.; Butterfield, S. Effect of Turbulence Variation on Extreme Loads Prediction for Wind Turbines. *J. Sol. Eng.* **2002**, *124*, 387–395.

28. Blum, J.R.; Kiefer, J.; Rosenblatt, M. Distribution free tests of independence based on the sample distribution function. *Ann. Math. Stat.* **1961**, *32*, 485–498.

29. Naess, A.; Haug, E. Extreme Value Statistics of Wind Speed Data by the POT and ACER Methods. *J. Offshore Mech. Arct. Eng.* **2010**, *132*, 041604.

30. Efron, B.; Tibshirani, R.J. *An Introduction to the Bootstrap*; Chapman and Hall: New York, NY, USA, 1993.